

# Investigation of the Proton-Assisted Pathway to Formation of the Catalytically Active, Ferryl Species of P450s by Molecular Dynamics Studies of P450eryF

Danni L. Harris\* and Gilda H. Loew

Contribution from the Molecular Research Institute, 845 Page Mill Road,  
Palo Alto, California 94304

Received December 6, 1995. Revised Manuscript Received April 8, 1996<sup>⊗</sup>

**Abstract:** The recently determined crystal structure of cytochrome P450eryF (6-deoxyerythronolide B hydroxylase; CYP107A1) in its ferric heme substrate-bound form has been used to address one of the most fundamental unresolved aspects of the mechanism of oxidation common to this ubiquitous family of metabolizing heme proteins, the pathway from the twice reduced dioxygen species to the putative catalytically active ferryl oxygen species. Both of these species are too transient to have been characterized experimentally, and the transformation from one to the other has been only partially characterized. The observed requirement of two protons and the formation of water in this transformation suggests a proton-assisted dioxygen bond cleavage as a plausible pathway. However, this pathway is difficult to establish by experiment alone, and the source of the protons in the largely hydrophobic binding pocket of the P450s remains unclear. In this work we have performed molecular dynamics simulations of the twice reduced dioxygen substrate-bound form of this isozyme in order to (i) determine the plausibility of the proposed pathway to compound I formation, a proton-assisted cleavage of the dioxygen bond, and (ii) investigate the possible source of these protons. The analysis of the molecular dynamics trajectories of this species does indeed provide further evidence for this pathway and points to a source of protons. Specifically, two dynamically stable hydrogen bonds to the distal oxygen atom of the dioxygen ligand, one by the substrate and the other by a bound water, are found, consistent with the proposed proton-assisted cleavage of the bond and formation of water. In addition, an extensive dynamically stable hydrogen bond network is formed that connects the distal oxygen to Glu 360, a well-conserved residue in a channel accessible to solvent that could be the ultimate source of protons. The simulations were done for both a protonated and unprotonated Glu and led to a proposed mechanism of proton transfer by it to the distal oxygen atom. In order to validate the procedures used for the simulation of this transient twice-reduced species, we have used these same procedures to perform molecular dynamics simulations of two other forms of P450eryF, the ferric and ferryl substrate-bound species, and compared the results with experiment. The results for the ferric substrate-bound species were assessed by comparisons to the experimentally determined X-ray structure and fluctuations, and good agreement was found. The simulations performed for the ferryl substrate-bound species led to the correct prediction of the observed regio- and stereospecific hydroxylation of its natural substrate, 6-deoxyerythronolide B (6-DEB) at the 6S position. The results of these two additional studies lend credibility to the important mechanistic inferences from the simulations of the transient twice reduced dioxygen species: further evidence for a proton-assisted pathway from it to the catalytically active ferryl species and a possible source of the protons.

## Introduction

Cytochrome P450eryF (CYP107A1) is a member of the ubiquitous cytochrome P450 family containing over 250 known isozymes that catalyze the monooxygenation of a diverse set of substrates. In particular, cytochrome P450eryF catalyzes the hydroxylation of 6-deoxyerythronolide B (6-DEB) at the 6S position, a necessary step in the synthesis of erythromycin. The crystal structure of the ferric substrate-bound cytochrome P450eryF has been reported recently,<sup>1</sup> and the binding affinity and enzymatic kinetics of 6-deoxyerythronolide and numerous related substrates have been determined.<sup>2</sup> This is only the second member of the ubiquitous P450 family of isozymes for which a substrate-bound crystal structure has been determined. It thus provides a unique opportunity to further examine the proposed relationships between P450 structure and function

based up to now primarily on the known structure of one substrate-bound isozyme, P450cam (CYP101).<sup>3</sup>

All cytochrome P450s share a common structural feature of the enzymatic active site: a nearly planar ferric–protoporphyrin IX heme complex, in which the iron is attached via a “proximal” cysteinate linkage to the remainder of the protein, forming a portion of the enzymatic active site. A “distal” pocket on the other side of the heme unit provides a variable spin and oxidation state site at which the substrate and molecular oxygen bind and the substrate is transformed to products via a variety of oxygen insertion reactions.

In addition to a common prosthetic group, all cytochrome P450s are believed to share a common enzymatic cycle for transformation from the resting state to the catalytically active state as well as a common mode of oxidation by transfer of a single active oxygen atom from it to substrates. This common enzymatic cycle is shown in Figure 1. These steps are (1) substrate binding, (2) one electron-reduction, (3) binding of molecular oxygen, (4) a second electron reduction and addition

<sup>⊗</sup> Abstract published in *Advance ACS Abstracts*, June 15, 1996.

(1) Cupp-Vickery, J. R.; Poulos, T. L. Structure of cytochrome P450eryF involved in erythromycin biosynthesis. *Struct. Biol.* **1995**, *2*, 144–153.

(2) Andersen, J. F.; Tatsuta, K.; Gungi, H.; Ishiyama, T.; Hutchinson, C. R. Substrate Specificity of 6-Deoxyerythronolide B Hydroxylase, a Bacterial Cytochrome P450 of Erythromycin A Biosynthesis. *Biochemistry* **1993**, *32*, 1905–1913.

(3) Poulos, T. L.; Finzel, B. C.; Howard, A. J. *J. Mol. Biol.* **1987**, *195*, 687–700.

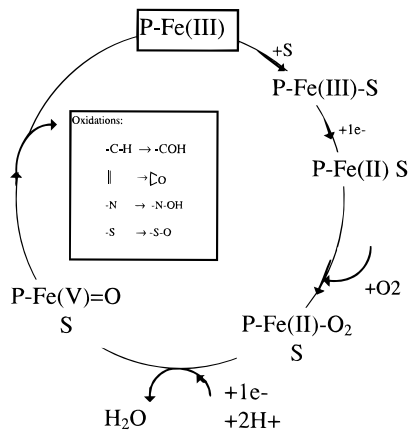


**Figure 1.** Enzymatic cycle for hydroxylation common to all P450s.

of two protons, (5) the formation of the putative ferryl oxygen catalytically active species, and (6) transfers of the active oxygen atom to substrates by a variety of oxygen insertion paths leading to product and a return to the resting state of the enzyme, the first step in the cycle. The elucidation of the nature of the species in the cycle beginning with the formation of the twice reduced species is experimentally challenging because the reaction proceeds rapidly from the transient twice-reduced dioxygen species to the transient active oxygen species and then to products. However, although both the twice reduced dioxygen species and the active oxygen species are very transient, recent experimental studies have reported ESR spectra<sup>4</sup> attributed to the twice-reduced species and electronic spectra attributed to these two transient species.<sup>5,6</sup> In addition, recent density functional calculations have revealed that (1) the optimized structures of the once and twice reduced dioxygen bound heme species are very similar and (2) the twice reduced dioxygen species is indeed a stable entity.<sup>7</sup>

In addition to the nature of the transient species, another long unresolved question is the mechanism of formation of the catalytically active species. Current evidence, including isotope substitution kinetic data<sup>8</sup> and an observed solvent kinetic isotope effect,<sup>9</sup> is consistent with formation of a compound I/radical-cation ferryl oxygen transfer species, similar to the species found in peroxidases, from the twice reduced dioxygen species in a step requiring two protons. This proton-assisted step is partially rate limiting to the overall reaction and leads to the formation of water. Taken together, these results imply a proton-assisted dioxygen bond cleavage pathway from the twice reduced dioxygen species to the ferryl species shown schematically in Figure 2. This figure shows a concerted version of this pathway that proceeds through a transition state involving simultaneous addition of protons to the distal oxygen and dioxygen bond cleavage. However, subtle variations of this proton-assisted mechanism are also possible, involving different extents of concertedness of these three steps. It is very difficult to further characterize this pathway experimentally. Moreover, in the

(4) Davydov, R.; Kappl, R.; Huttermann, J.; Peterson, J. A. EPR-Spectroscopy of Reduced Oxy-ferrous P450cam. *FEBS Lett.* **1991**, *295*, 113.

(5) Kobayashi, K.; Iwamoto, T.; Honda, K. Spectral Intermediate in the reaction of the Ferrous Cytochrome P450cam with super-oxide anion. *Biochem. Biophys. Res. Commun.* **1994**, *201*, 1348.

(6) Egawa, T.; Miki, H.; Ogura, T.; Makino, R.; Ishimura, Y.; Kitagawa, T. Observation of the Fe<sup>IV</sup>=O stretching Raman band for a thiolate-ligated heme protein. *FEBS Lett.* **1992**, *305*, 206–208.

(7) Komornicki, A.; Loew, G. In preparation.

(8) (a) Atkins, W. M.; Sligar, S. G. *Biochemistry* **1988**, *27*, 1610–1616.

(b) Jones, J. P.; Rettie, A. E.; Trager, W. F. *J. Med. Chem.* **1990**, *33*, 1242–1246.

(9) Aikens, J.; Sligar, S. *J. Am. Chem. Soc.* **1994**, *116*, 1143–1144.

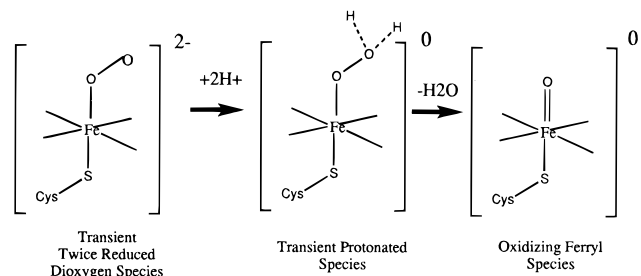


**Figure 2.** Proposed proton-assisted pathway to formation of compound I from the twice reduced dioxygen bound species.

largely hydrophobic binding pocket, typical of P450s, the origin of the protons is not clear.

Polar and charged residues often play a functional role either in stabilizing enzymatic intermediates via hydrogen bonding or in actual proton-assisted cleavage of bonds or functional groups. For this reason, several studies of cytochrome P450cam have focused on determining the effect of amino acid substitutions for Thr 252,<sup>10–12</sup> a residue in the dioxygen binding pocket thought to play a role in the stabilization of the dioxygen bound state, and for Asp 251,<sup>13–16</sup> a residue thought to be a proton source in compound I formation from the twice reduced dioxygen species. Some mutation data indicates the requirement of a hydrogen-bonding amino acid (such as Thr or Ser) at position 252<sup>10,11</sup> and an acidic residue at position 251 for proper function.<sup>15,16</sup> A critical evaluation of cytochrome P450cam mutational data, however, indicates some exceptions to these patterns, e.g., where a methoxythreonine-252 substituted for Thr 252<sup>12</sup> or aliphatic residues substituted for Asp 251<sup>15,16</sup> still result in efficient compound I formation and hydroxylation of substrates. While such exceptions do not exclude some role of these particular polar or acidic residues in the determination of the course of compound I formation, they do, however, indicate that the enzyme can achieve stabilization of the dioxygen bound state or proton-assisted cleavage of the dioxygen bond via other residues or bound waters in the binding-site region.

Four known structures of P450 isozymes have now been solved: P450cam in its substrate-bound form,<sup>3</sup> P450-BM3 (CYP102)<sup>17,18</sup> and P450terp (CYP108)<sup>19</sup> in their substrate-free forms, and P450eryF in its substrate-bound form.<sup>1</sup> The structures of these four isozymes were examined for the extent of conservation of polar and acidic residues in the region of the binding-site cavity. Figure 3 shows a superposition of these four known crystal structures aligned with respect to their heme units. We see from this figure that Asp 251, in P450cam, is either conserved or transformed to the closely related Glu and that Glu 366 (in P450cam) is completely conserved in the other P450 isozymes of known structure.

(10) Martinis, S. A.; Atkins, W. M.; Slayton, P. S.; Sligar, S. G. *J. Am. Chem. Soc.* **1989**, *111*, 9252–9253.

(11) Imai, T.; Schimada, H.; Watanabe, Y.; Matsushima-Hibiya, Y.; Makino, R.; Koga, H.; Horiuchi, T.; Ishimura, Y. *Proc. Natl. Acad. Sci. U.S.A.* **1989**, *86*, 7823–7827.

(12) Kimata, Y.; Shimada, H.; Hirose, T.; Ishimura, Y. *Biochem. Biophys. Res. Commun.* **1995**, *208*, 96–102.

(13) Gerber, N. C.; Sligar, S. G. *J. Biol. Chem.* **1994**, *269*, 4260–4266.

(14) Gerber, N. C.; Sligar, S. G. *J. Am. Chem. Soc.* **1992**, *114*, 8742–8743.

(15) Shimada, H.; Makino, R.; Imai, M.; Horiuchi, T.; Ishimura, Y. In *International Symposium on Oxygenases and Oxygen Activation*; Yamamoto, S., Nozaki, M., Ishimura, Y., Eds.; Yamada Science Foundation: Hachioji, Japan, 1991; pp 133–136.

(16) Y. Ishimura, private communication.

(17) Ravichandran, K. G.; Boodupalli, S. S.; Hasemann, C. A.; Peterson, J. A. *Science* **1993**, *261*, 731–736.

(18) Li, H.; Poulos, T. L. *Acta Crystallogr. D* **1995**, *51*, 21–32.

(19) Haseman, C. A.; Ravichandran, K. G.; Peterson, J. A.; Deisenhofer, J. **1994**, *236*, 1169–1185.

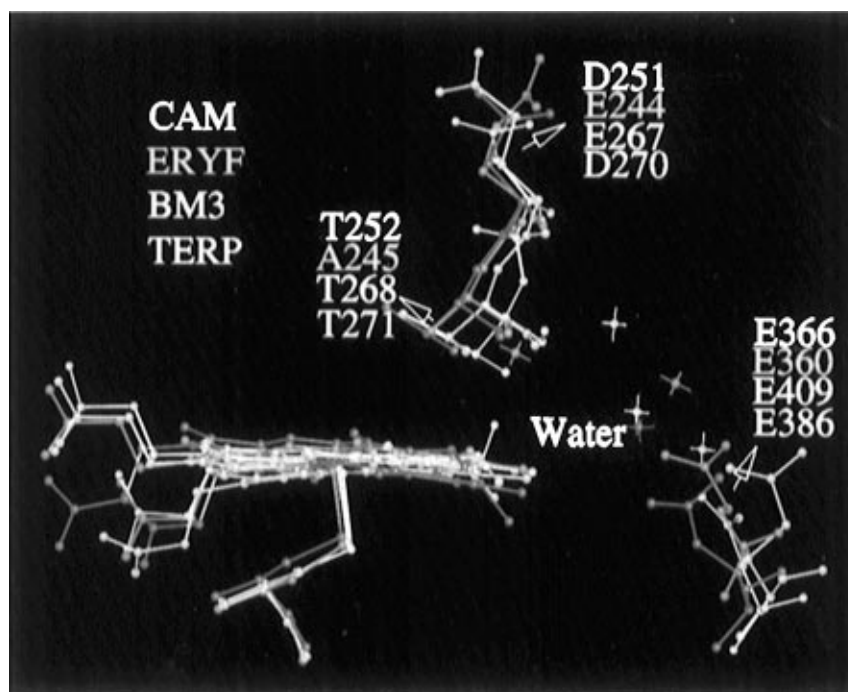


**Figure 3.** Superposition of four known crystal structures aligned with respect to their heme: P450*cam* (CYP101), P450-BM3 (CYP102), P450*terp* (CYP108), and P450*eryF* (107A1).

This superposition illustrates that the conserved Glu is another possible key residue in the formation of compound I, a role inferred directly from the X-ray structure of the substrate-bound P450*cam*.<sup>3</sup> In this crystal structure, Glu 366 is part of a contiguous hydrogen bond network involving several bound waters in a buried solvent channel leading to Thr 252. It is thus possible that it may be a conduit for proton transfer to the terminal oxygen in the twice reduced dioxygen bound state of P450*cam*. In three out of these four enzymes with known structures there also appear to be a number of waters present leading from the acidic glutamate toward the binding-site cavity. This hypothesis has not, however been assessed by any experimental mutation studies involving Glu 366.

Surprisingly, Thr 252, for which there is the most robust evidence for requirement for compound I formation in P450*cam*, while conserved in P450-BM3 and P450*terp* is replaced by an Ala 245 in P450*eryF*. This particular substitution in P450*eryF* is even more unexpected since the T252A mutant in P450*cam* prevents compound I formation. These results dramatically illustrate how a variation in a residue at a given position within one isozyme cannot always be inferred to have the same effect on function as the same variation in the consensus position of another isozyme, even if, as is the case here, the residue is in the most conserved secondary structure motif of all the P450s, the I helix.

In the work reported here, using the recently determined X-ray structure of substrate-bound P450*eryF*,<sup>1</sup> we have addressed the important unresolved aspect of the postulated common enzymatic cycle just described, the mechanism of formation of the putative active oxygen species from the twice reduced dioxygen form. Molecular dynamics simulations of cytochrome P450*eryF* in the substrate-bound twice reduced dioxygen species have been performed to further examine two specific aspects of the mechanism of formation of compound I: (1) the plausibility of the proton-assisted pathway of dioxygen bond cleavage of the twice reduced dioxygen species and (2) the possible source and mechanism of transfer of these protons to the distal oxygen atom. Although the schematic pathway in Figure 2 depicts simultaneous formation of two H-bonds to the distal oxygen

atom, the simulations performed were not biased to either single or concerted hydrogen bonding. The property that has been examined to address these questions is the extent to which a dynamically robust hydrogen network leading from the distal oxygen to Glu 360 is obtained. The presence of such a network is taken as evidence for the existence of a precursor reactant complex consistent with a proton-assisted dioxygen bond cleavage. A detailed characterization of the remainder of the pathway involving proton transfer and dioxygen bond cleavage involves use of quantum mechanical methods and was not addressed in this study. The simulations were done for both a protonated and an unprotonated Glu and led to a proposed mechanism of proton transfer by it to the distal oxygen atom. Finally, as further validation steps we have examined the dynamic behavior of this enzyme in the ferric–heme and ferryl–oxygen–heme bound states and used the latter simulation to predict the preferred hydroxylation of the 6-DEB substrate for comparison with known experimental results, using previously established methodology for prediction of observed stereo- and regioselective oxidation of a variety of substrates.<sup>20,21</sup>

## Methods

The initial structures for the three species of the P450*eryF* isozyme considered in this study were obtained using the recently determined crystal structure of the substrate-bound ferric cytochrome P450*eryF* and included all crystallographically observed bound water. All simulations were performed using AMBER 4.1,<sup>22</sup> which has undergone extensively revised parametrization from previous versions, including

(20) Harris, D. L.; Loew, G. H. *J. Am. Chem. Soc.* **1995**, *117*, 2738–2746.

(21) (a) Collins, J. R.; Camper, D. L.; Loew, G. H. *J. Am. Chem. Soc.* **1991**, *113*, 2736–2743. (b) Chang, Y.-T.; Loew, G. H.; Rettie, A. E.; Baillie, T. A.; Sheffels, P. R.; Ortiz de Montellano, P. R. *J. Quantum Biol. Symp.*, in press. (c) Fruetel, P. R.; Collins, J. R.; Camper, D.; Loew, G.; Ortiz de Montellano, P. R. *J. Am. Chem. Soc.* **1992**, *114*, 6987–6993. (d) Fruetel, J.; Chang, Y. T.; Collins, J.; Loew, G. H.; Ortiz de Montellano, P. R. *J. Am. Chem. Soc.* **1994**, *116*, 11643–11648. (e) Paulsen, M. D.; Bass, M. B.; Ornstein, R. L. *J. Biomol. Struct. Des.* **1991**, *9*, 187–203. Paulsen, M. D.; Ornstein, R. L. *J. Comput.-Aided Mol. Des.* **1992**, 449–460. (g) Bass, M. B.; Ornstein, R. L. *J. Comput. Chem.* **1993**, *14*, 541–548. (h) Paulsen, M. D.; Ornstein, R. L. *Protein Eng.* **1993**, *6*, 359–365.

**Table 1.** Charges Derived for Iron and Ligands from Semiempirical INDO/S Calculations of Four Heme Species

atom	charges <sup>a</sup>			
	ferric-heme species	once reduced dioxygen species	twice reduced dioxygen species	ferryl species
S	-0.860	-0.79	-0.89	-0.65
Fe	1.38	1.44	1.29	1.50
O1		-0.26	-0.38	-0.84
O2		-0.45	-0.48	
spin state system	sextet	singlet	doublet	quartet

<sup>a</sup> Mulliken charges on atoms for the heme species indicated, derived from INDO/S semiempirical calculations. The INDO/S state corresponding the calculated ground state spin multiplicity is also indicated.

substantial amino acid charge reparametrization based on RESP<sup>23</sup> fits to optimized 6-31G\* ab initio results. The charge parametrization of the eryF substrate was obtained by fitting atomic charges (a CHELPG fit) to the molecular electrostatic potential surface derived from a single-point 6-31G\*\*/3-21G\* calculation using Gaussian 92.<sup>24</sup> The convergence criteria employed for the 3-21G\* optimized geometry of this large flexible molecule was less stringent than the defaults for small molecules. However, it was additionally ascertained that only minor changes in the CHELPG<sup>25</sup> charge description for the substrate resulted from additional optimization steps. The remainder of the substrate vibrational and nonbonded van der Waals parameters was taken from the standard AMBER parameter database.

The charges for the heme unit in the three different forms relevant to the work reported here, the ferric-heme, the twice reduced oxygen bound heme, and the ferryl-oxygen bound heme, were derived from INDO-ROHF type calculations of Mulliken atomic charges. This source of net atomic charges has been used in all of our heme protein simulations. It has not yet been possible, given the computational resources and state of the art of quantum chemical calculations for these large systems, to use charges derived from fits to ab initio calculation of molecular electrostatic potentials for these systems. Ab initio DFT studies of iron heme systems in progress, however, indicate charge descriptions that are qualitatively similar to those obtained from INDO-ROHF type calculations of Mulliken atomic charges, namely, identical charges on the oxygen atoms of the dioxygen species but slightly smaller charges on the iron and carbon centers.<sup>26</sup>

The INDO/S derived Mulliken charges on the iron and its S and O ligands are shown in Table 1 for four heme species: the ferric, once and twice reduced dioxygen bound, and compound I heme species. The spin state of the ligand-heme system determined to be the electronic ground state for each species is also reported. As can be inferred by the heteroatom charges shown, much of the added electron density in both the first and reduction steps is distributed in a delocalized fashion in the porphyrin system. Thus, for example, the charges on the S, O1 (proximal dioxygen atom), and O2 (terminal dioxygen atom) atoms in twice-reduced species reflect only a moderate increase in negative charge density on these centers and a commensurate reduction of positive charge on the Fe compared to the once reduced dioxygen species, the remainder of the charge being distributed over the porphyrin ring. Such characteristics of the charge distribution are also reflected in the density functional calculations we have performed on these species.<sup>26</sup>

The internal force constant parametrization for the twice reduced dioxygen complex was taken to be the same as for the once reduced

dioxygen bound state, in the absence of any direct spectroscopic information regarding the stretching and bending force constants for this species. The parametrization of the ferryl state was as previously described.<sup>20</sup>

Hydrogen atoms were added to the heavy atoms in the P450eryF crystal structure, including all crystallographic waters. All glutamic and aspartic residues were deprotonated, and lysine and arginine residues were protonated. This assumption is reasonable given that most of these residues either are found to be involved in buried salt bridges or are found to be present on the surface of the enzyme. In a second simulation of the twice reduced dioxygen species, Glu 360 was protonated in order to examine if and how such a transient form of this species could play a proposed role in proton donation to the distal oxygen atom. The protonation sites of the histidine residues were assigned on the basis of proximity of acidic/basic residues within a 4 Å radius of the histidine nitrogens. For each of the three substrate-bound species characterized, (i) the ferric form, (ii) the twice reduced dioxygen bound form, and (iii) the ferryl form, the corresponding heme unit was constructed and used in the full protein simulations.

Each of the three substrate-bound P450 structures included in this study was energy minimized using AMBER 4.1 using 100 steps of steepest descents followed by sufficient steps of conjugate gradients to reduce the gradient to  $\approx 0.8$  kcal/Å. The positions of the hydrogen atoms attached to oxygen and nitrogen were then modified by short dynamics runs of 5–10 ps at 350 K. The structure was equilibrated for 15 ps at 300 K by loosely coupling the system to a heat bath and employing a series of gradually decreasing harmonic coordinate constraints. The system was then further equilibrated for about 25 ps before accumulation of dynamics data for analysis. Following the equilibration procedure, molecular dynamics runs were continued for 125–150 ps. Nonbonded interactions were truncated at a relatively long distance of 13.0 Å in order to minimize the large forces associated with truncations in the nonbonded interactions. In these studies, we have employed a radially dependent dielectric constant of  $D = r$ , where  $r$  is the interatomic distance for the atom pair electrostatic contribution being computed, in lieu of including an explicit solvent hydration shell. While this approximation lacks a rigorous physical basis, its use has been shown to prevent artifactual contractions during simulations of cytochrome P450 with known structures.<sup>27</sup> We have determined if this approximation used in these studies also prevented these artifactual consequences.

**Criteria Used for Prediction of Regiospecific Hydroxylations.** As in past studies, the most widely accepted mechanism of substrate hydroxylation by P450s was used to select the criteria for prediction of regiospecific hydroxylation of the DEB substrate by P450eryF. This mechanism involves hydrogen atom abstraction by the active oxygen atom of the ferryl species followed by radical recombination to produce the hydroxylated products. The steric criteria used were the distance of each H atom of the substrate from the ferryl oxygen and the Cn-Hn-OFe angle. Structures were saved at time intervals of 0.25 ps during the molecular dynamics simulations of the substrate-bound ferryl species. These structures were used to calculate relevant distances and angles and to obtain the number of times that each substrate hydrogen atom was  $\leq 3.5$  Å from the ferryl oxygen with an H-bond angle of  $180 \pm 45^\circ$ . The percentage of the total sampled time frames for which each Hn fulfilled this criterion was used as the steric determinant to predict the percentage hydroxylation product formed at this position. This is the same steric criterion used in all our previous studies predicting regiospecific hydroxylation of substrates by P450cam. In addition, for those sites for which the steric criteria predicted some percent hydroxylation, the relative stability of the radical formed at each of these sites was calculated using an AM1 Hamiltonian in the Gaussian94/DFT<sup>28</sup> program. This quantity was used as a second, thermodynamic/electronic, criterion for selective hydroxylation, as was also done in our past studies of P450cam hydroxylations.<sup>20,21</sup> In previous studies using compounds with known relative radical energies,

(22) Cornell, W. D.; Cieplak, P.; Bayly, C. I.; Gould, I. R.; Merz, K. M., Jr.; Ferguson, D. M.; Spellmeyer, D. D.; Fox, T.; Caldwell, J. W.; Kollman, P. A. *J. Am. Chem. Soc.* **1995**, *117*, 5179–5197.

(23) Bayly, C. I.; Cieplak, P.; Bayly, C. I.; Kollman, P. A. *J. Phys. Chem.* **1993**, *97*, 10269–10280.

(24) Gaussian 92, Revision C: M. J. Frisch, G. W. Trucks, M. Head-Gordon, P. M. W. Gill, M. W. Wong, J. B. Foresman, B. G. Johnson, H. B. Schlegel, M. A. Robb, E. S. Replogle, R. Gomperts, J. L. Andres, K. Raghavachari, J. S. Binkley, C. Gonzalez, R. L. Martin, D. J. Fox, D. J. Defrees, J. Baker, J. J. P. Stewart, J. A. Pople; Gaussian, Inc., Pittsburgh, PA, 1992.

(25) Breneman, C. M.; Wiberg, K. W. *J. Comput. Chem.* **1990**, *11*, 361.

(26) A. Komoricki, private communication.

(27) Harris, D. L.; Loew, G. H. *J. Am. Chem. Soc.* **1995**, *117*, 2738–2746.

(28) Gaussian 94, Revision B.1: M. J. Frisch, G. W. Trucks, H. B. Schlegel, P. M. W. Gill, B. G. Johnson, M. A. Robb, J. R. Cheeseman, T. Keith, G. A. Petersson, J. A. Montgomery, K. Raghavachari, M. A. Al-Laham, V. G. Zakrzewski, J. V. Ortiz, J. B. Foresman, J. Cioslowski, B.

we have compared estimates of relative radical energies obtained using the AM1 Hamiltonian and using *ab initio* calculations with Gaussian split-valence basis sets with experimental results. These comparisons indicated that using an AM1 Hamiltonian in G94, like those obtained using MOPAC,<sup>29</sup> produced the same relative order of radical stabilities as the *ab initio* results but tended to overestimate the radical energy differences by at least a factor of 2. Since this level of accuracy is sufficient to evaluate the effect of radical stability on preferred product formation, an AM1 Hamiltonian was thus used here to estimate the thermodynamic component modulating competing 6-DEB substrate hydrogen abstractions to use together with the steric criteria to predict hydroxylation profiles. Validation of the combined use of these steric and thermodynamic criteria for predictions of selective hydroxylation has been thoroughly examined in other benchmark studies.<sup>20,21</sup>

## Results and Discussion

**Ferric–Heme Substrate-Bound P450eryF.** In order to validate the procedures used for the transient substrate-bound, twice reduced dioxygen cytochrome P450eryF species, a molecular dynamics (MD) simulation was performed for the substrate-bound ferric–heme form, including crystallographic waters, using the same procedures, and the results were compared with the crystallographic results. The RMS deviations of the MD average structure of the protein from the crystal and energy minimized crystal structure were 2.01 and 1.92 Å, respectively, for all heavy atoms including water. These RMS deviations were 1.68 and 1.42 Å, respectively, excluding water, indicating that the secondary and tertiary protein structures are well conserved during the simulation. The RMS difference between the optimized substrate heavy atom positions and the MD average coordinates of the substrate is 0.17 Å.

Comparison of the computed and experimental *B*-factor indicates general qualitative agreement with the possible exception of a surface loop near residue 260 lacking any significant nonbonded contacts from other secondary structural elements or explicit solvation. The calculated substrate 6-DEB *B*-factor was 16 Å<sup>2</sup>, in good agreement with the crystal structure isotropic *B*-factor value of 17.2 Å<sup>2</sup>.

The temporal profiles of both the radius of gyration and total number of hydrogen bonds were also monitored during the simulation. The radius of gyration of the P450eryF showed only minor deviations from the MD average value of 19.7 Å during the simulation, remaining in good agreement with the crystal structure value of 20.9 Å. The similarity in value and relative constancy of the radius of gyration of the protein indicate the lack of artifactual shrinkage. The number of hydrogen bonds was also well conserved during the simulation, fluctuating between the initial value of 810 to a final value of 830 at the end of the production dynamics. Thus the use of a radially dependent dielectric constant in the absence of explicit solvation, although without a rigorous foundation, nevertheless eliminates artifactual protein contraction with no apparent deleterious effect on the temporal evolution of hydrogen-bonding patterns beginning with the crystal structure, a concern in the use of this approximation.

These combined results indicate good agreement between experimental and simulated structure and fluctuations and provide validation of the parametrization, simulation conditions, and approximations employed for the characterization of the other substrate-bound P450eryF enzymatic species based upon the substrate-bound ferric heme crystal structure.

Figure 4a shows the substrate-bound binding-site cavity of the P450eryF enzyme after 125 ps of simulation. This substrate (Figure 4b) is much larger and contains more polar groups than camphor, the natural substrate of cytochrome P450cam. It is composed of 21 carbons, 6 oxygens, and 21 hydrogens in a complex 14-membered ring. Yet, as shown in Figure 4a, in common with P450cam, the substrate binds in a buried, largely hydrophobic pocket near the heme, making numerous van der Waals contacts with hydrophobic residues lining the substrate cavity, specifically A74, Y75, F78, F86, N89, G91, T92, I174, L175, R185, V237, L240, A241, G242, E244, A245, P288, L391, and L392. In addition, as shown in Figure 5, a dynamically stable hydrogen bond network is found leading from the substrate to Glu 360. It is seen that the polar hydroxyl and keto groups of the substrate are connected through hydrogen bond bridging networks to the rest of the protein. Specifically the C5 and C11 hydroxyl groups and the C9 keto group are hydrogen bonded to the enzyme via mediating waters, and multiple simulations of this form of the enzyme indicate that the C3-OH transiently hydrogen bonds to the carbonyl oxygen of Leu240. The coordinate frame shown is that corresponding to the end of the ferric–heme–substrate-bound simulation. This hydrogen network is established shortly following energy minimization and MD equilibration and persists throughout the simulation.

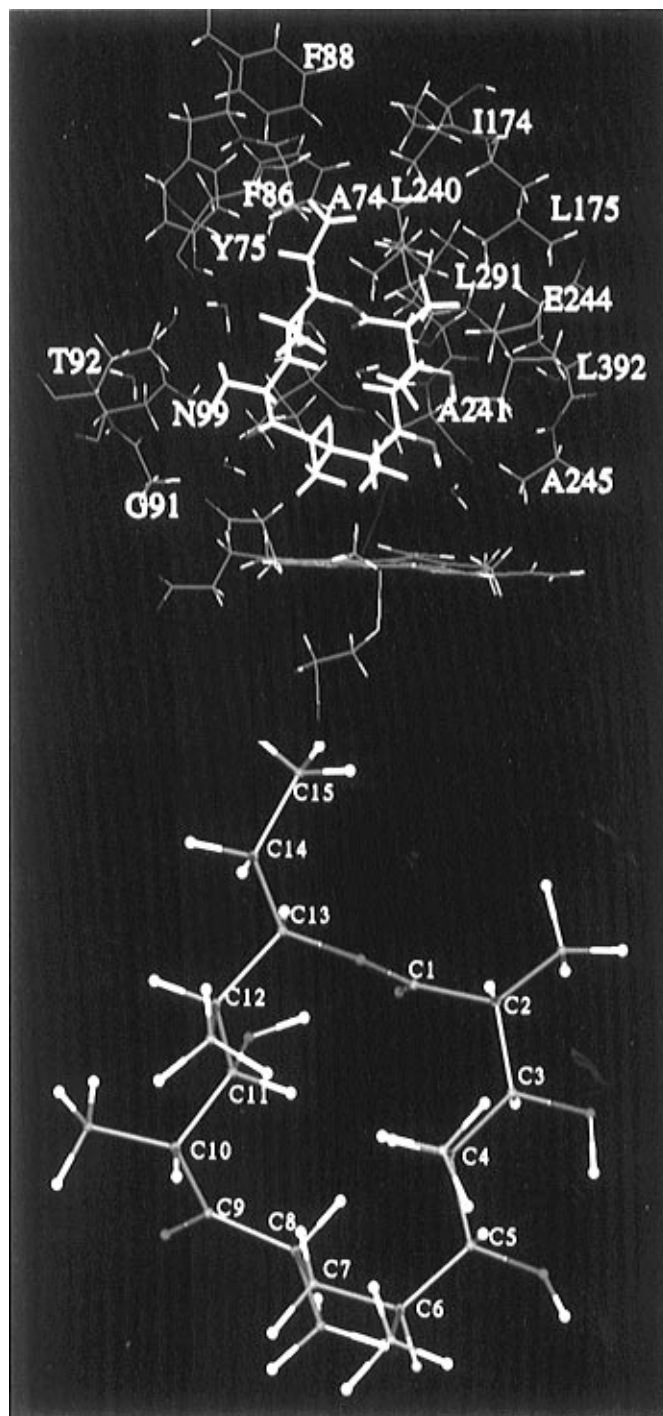
**Twice Reduced Dioxygen Substrate-Bound State.** The main goal of this study was the characterization of this transient species to determine if its energy-optimized structure and simulated dynamic behavior provide any additional evidence for the validity of the proton-assisted dioxygen bond cleavage mechanism of formation of compound I from it, shown schematically in Figure 2. As described in Methods, since a structure of this transient species was lacking, it was constructed from the known structure of the substrate-bound ferric form, by the addition of the dioxygen ligand and use of the calculated net atomic charges and other parameters for this species. This is the first time that a simulation of this species has been reported.

The results obtained provide clear evidence for the presence of an extensive hydrogen-bonding network in the distal binding pocket of this twice reduced dioxygen substrate-bound isozyme following energy minimization and equilibration. As shown in Figure 6, 25 ps after equilibration of the optimized structure the terminal oxygen of the dioxygen ligand has two proton-donating partners: the C5-OH group of the 6-DEB and a bound water (crystallographic water 519). This formation of two stable hydrogen bonds to the terminal oxygen in the twice reduced dioxygen species, demonstrated for the first time by these simulations, provides direct support for the key step invoked in the proton-assisted pathway of dioxygen bond cleavage of the twice reduced dioxygen species to compound I formation (cf. Figure 2). Moreover, this H-bonding network extends from the terminal oxygen atom of the ligand, i.e., Fe–O1–O2 to H2O519 to Ala 241 to H2O564 to Ser 246 to Glu 360, a potential key residue in a proton relay pathway involving the ultimate source of protons.

While the presence of this H-bonded network early in the simulation is suggestive, the extent to which it is preserved during the MD simulations and to which it favors protonation of the distal over the proximal oxygen atom is crucial to the plausibility of the proton-assisted mechanism of compound I formation from this twice reduced dioxygen species. Figure 7 a–j shows the time dependence of the main hydrogen bonds connecting the bound dioxygen ligand ultimately to the Glu 360.

B. Stefanov, A. Nanayakkara, M. Challacombe, C. Y. Peng, P. Y. Ayala, W. Chen, M. W. Wong, J. L. Andres, E. S. Replogle, R. Gomperts, R. L. Martin, D. J. Fox, J. S. Binkley, D. J. Defrees, J. Baker, J. P. Stewart, M. Head-Gordon, C. Gonzalez, and J. A. Pople; Gaussian, Inc., Pittsburgh, PA, 1995.

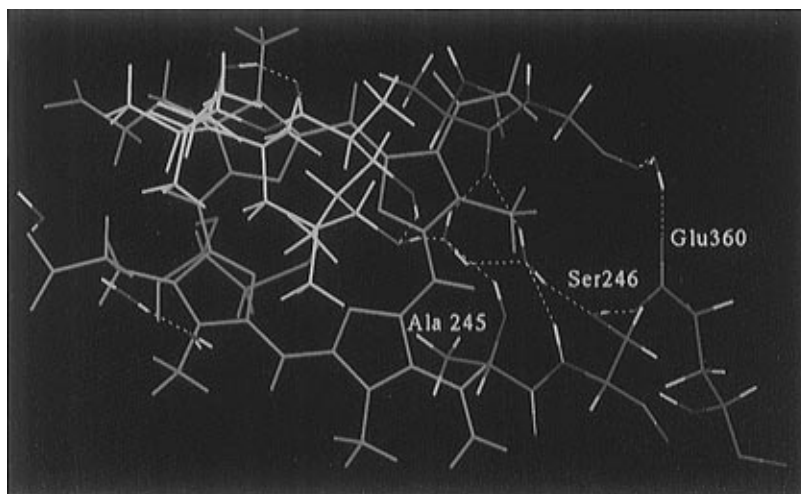
(29) Stewart, J. J., MOPAC 6.0, QCPE Program 455, Bloomington, IN.



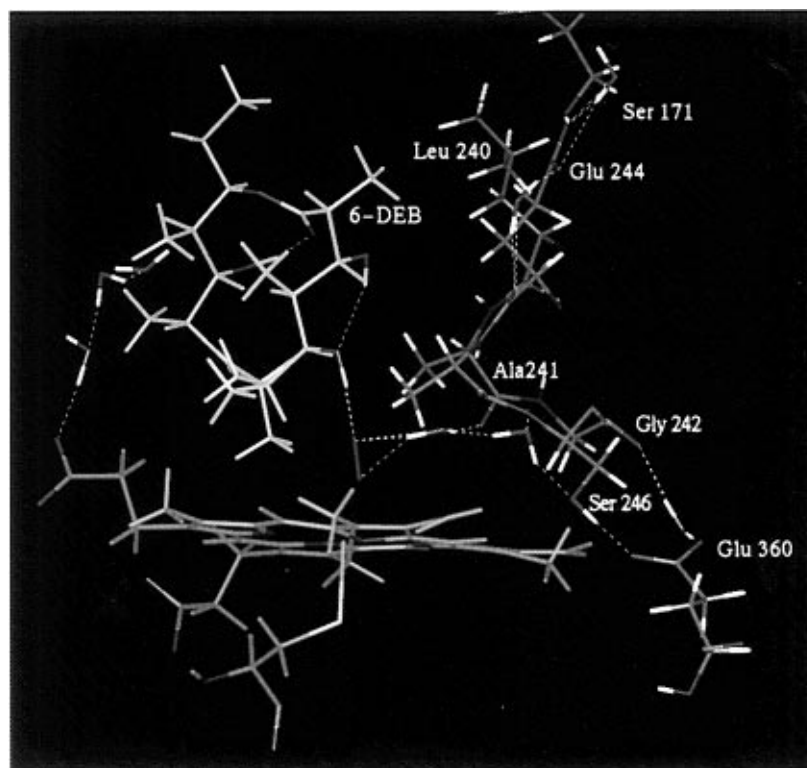
**Figure 4.** (a, top) Cytochrome P450eryF binding site in the substrate-bound ferric heme form after 125 ps of simulation showing all residues within 3.0 Å of the 6-DEB substrate (colored yellow with oxygens depicted in red). Note that Pro 288 is not shown in order to allow greater visibility of the substrate in the binding site. (b, bottom) 6-DEB P450eryF substrate. The carbon numbering scheme used and referred to in this work is depicted. The known experimentally determined site of completely regio- and stereospecific hydroxylation (at the 6S position) is highlighted in magenta.

Figure 7a–d shows the time dependent behavior of the H-bonds formed by the distal and proximal atoms of the dioxygen ligand with the substrate C5-OH and the H<sub>2</sub>O (519). Comparison of the hydrogen bond time series of H<sub>2</sub>O519 with the terminal (O2) and proximal oxygen (O1) atoms of the dioxygen ligand indicates that the bound water consistently favors a H-bond to the terminal oxygen (O2) and that this H-bond is stable during the simulation (Figure 7b,d). A similar examination of the time series for the 6-DEB C5-OH interactions with both the proximal (O1) and the terminal oxygen (O2) of the bound dioxygen also indicates a preferential interaction of the substrate C5-OH with the terminal oxygen (Figure 7a,c).

Examination of these two sorted time series in Figure 8 also shows a clear preference of the C5-OH with the terminal dioxygen atom (O2). In this figure, the distances of the C5-OH hydroxyl to both the O1 and O2 dioxygen atoms are sorted in order of increasing OH–O2 (terminal oxygen) distance with the corresponding OH–O1 (proximal oxygen) distance time series sorted by the same criteria. Examining this figure at any sorted point (abscissa value), we see that the substrate C5-OH is always closer to the terminal oxygen (O2) than to the oxygen attached to the iron (O1), since for any point on the O2 curve the corresponding point on the O1 curve is at a longer distance.



**Figure 5.** Dynamically stable hydrogen bond network in substrate-bound ferric heme P450eryF (after 125 ps of simulation) leading from Glu 360 through Ser 246, crystallographic water 564, Ala 241, and H2O519 (in the binding site cavity) to the C5-OH of the substrate. The view of this interaction is from above the distal side of the heme (shown in blue), the substrate 6-DEB has been colored yellow with its keto and hydroxyl oxygens highlighted in red.



**Figure 6.** View of the binding site and extended hydrogen bond network evident at 25 ps (following equilibration) in the twice reduced dioxygen substrate-bound cytochrome P450eryF simulation. The heme has been depicted in light blue with dark blue nitrogens, and the propionate and bound dioxygen atoms are shown in red. The substrate coloring scheme is as used in Figure 4.

The results presented in Figures 7a–d and 8 taken together clearly indicate the preference for two hydrogen bonds with the terminal oxygen, one with a cavity water and one with the substrate. The former is stable throughout the simulations (Figure 7b) and the latter C5-OH for roughly one-third of the total simulation (Figure 7a). Although these classical simulations cannot describe the actual dioxygen bond breaking process, the double hydrogen bonding found favoring the terminal oxygen corresponds to the geometry one would expect for the initial reaction complex in a putative proton-assisted dioxygen cleavage mechanism of formation of compound I. Also since the simulations are not biased (a priori) to either single or double hydrogen bonding, the results also suggest that simultaneous protonation of the distal oxygen is possible in this system. While

this result does not provide actual evidence of such a proton transfer event and facile O–O bond cleavage, it does identify the existence of a reactant species consistent with the proton-assisted mechanism for such a reaction. Detailed investigation of the subsequent proton transfer and bond-breaking steps requires quantum chemical investigations that await further methodological advances.

Figure 7e–j shows the time series for the remainder of the relevant H-bonds connecting Glu 360 with the terminal oxygen atom of the bound dioxygen and indicates the formation of a dynamically stable hydrogen bond network connecting them. This stable hydrogen-bonding network pattern can be traced in these panels from the water 519, a proton donor to the terminal oxygen ligands through Ala 241 to H2O564 to the Ser 246

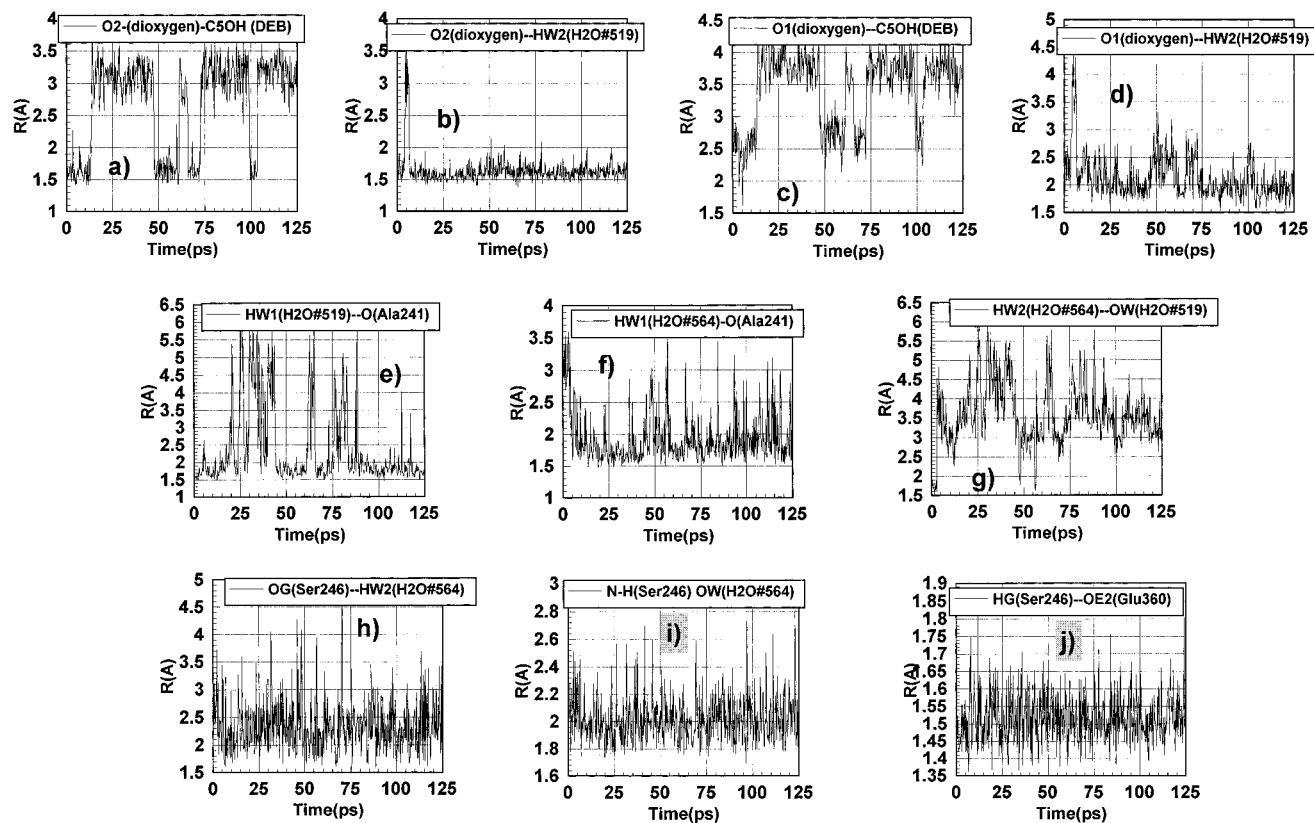


**Figure 7.** Distance time series reflecting short-range electrostatic interactions/hydrogen bonding in a network connecting Glu 360 to the heme bound dioxygen. Time series for cavity hydrogen bonds: (a) dioxygen atom O2— —HO-C5 (6-DEB); (b) dioxygen atom O2— —HW2(H2O#519); (c) dioxygen atom O1— —HO-C5 (6-DEB); (d) dioxygen atom O1— —HW2(H2O#519). Time series for hydrogen bonds leading to binding site: (e) HW1(H2O#519)— —O(Ala241); (f) HW1(H2O#564)— —O(Ala241); (g) HW1(H2O#564)— —OW(H2O#519); (h) OG(Ser246)— —HW2(H2O#564); (i) N-H(Ser246)— —OW(H2O#564); (j) HG(Ser246)— —OE2(Glu360).

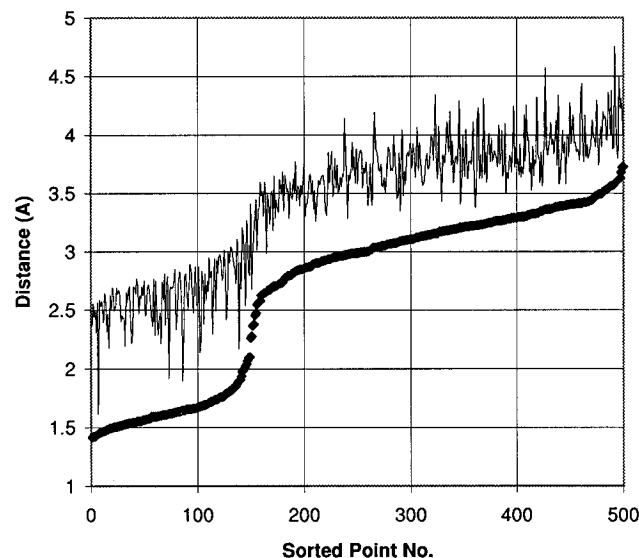


**Figure 8.** Competition between O1 and O2 of the dioxygen ligand for the C5-OH proton:  $\blacklozenge$ ,  $R(\text{O2-DEB-OH})$  Å;  $-$ ,  $R(\text{O1-DEB-OH})$  Å.

hydroxyl to the Glu 360 residue. In addition, H2O519 participates in transitory hydrogen-bonding interactions with H2O564. The stable hydrogen bond network exhibited in these time series could in principle serve as a conduit for proton transfer from the Glu 360 to the bound dioxygen and strongly indicates a plausible source of the protons.

Glu 360 is a highly conserved residue in the L helix of the four known P450 crystal structures. The L helix is surface exposed with most of its polar residues facing the solvent. The interior of this helix is largely hydrophobic with the striking

exception of Glu 360. The side chain of Glu 360 is a component of an interior solvent channel leading to the active site. Thus we propose that this side chain can serve as a molecular switch through which a proton from the solvent is ultimately transferred to the terminal oxygen atom in the following way. In the stable configuration characterized, in which one carboxyl oxygen of the ionized glutamate side chain is involved as a proton acceptor in the H-bonded network of the twice reduced dioxygen species, a proton could be transiently transferred to the second carboxylic oxygen. The side chain could then rapidly and freely rotate, allowing the protonated carbonyl group to become a proton donor in this H-bonded network to the terminal oxygen atom, and returning the system to its original state.

The feasibility of the switching mechanism proposed for proton transfer, involving the alternating role of the Glu 360 side chain as a proton donor and acceptor, rests heavily on the maintenance of a robust H-bonded network with this proposed transient protonated form of Glu 360, so that it can act as an efficient proton donor. To examine this possibility we have used the same procedures described above, to simulate the WT P450eryF in the twice reduced dioxygen bound form with Glu 360 in the protonated form. We have analyzed the MD trajectory, using the same criteria as in Figures 7a–j and 8 for the unprotonated form, for the presence and stability of a structure involving preferential double protonation of the terminal dioxygen ligand atom and a robust H-bonded network leading from there to the protonated form of the Glu. Figure 9 is a coordinate frame at 50 ps in the 150 ps simulation of the protonated Glu 360 twice reduced dioxygen bound P450eryF. This structure clearly indicates that, as in the unprotonated form, there are preferentially two-hydrogen bonds to the terminal oxygen atom of the ligand from the bound water 519 and the



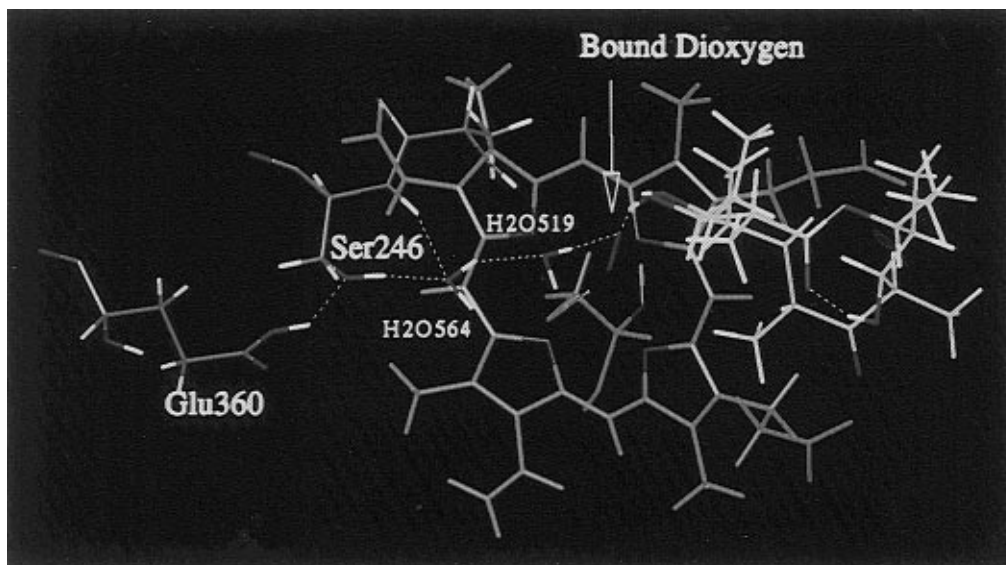


**Figure 9.** A 50 ps coordinate frame depicting the hydrogen-bonding pattern prevalent in the simulation of the protonated Glu 360 form of the enzyme in the twice reduced dioxygen substrate-bound P450eryF species.

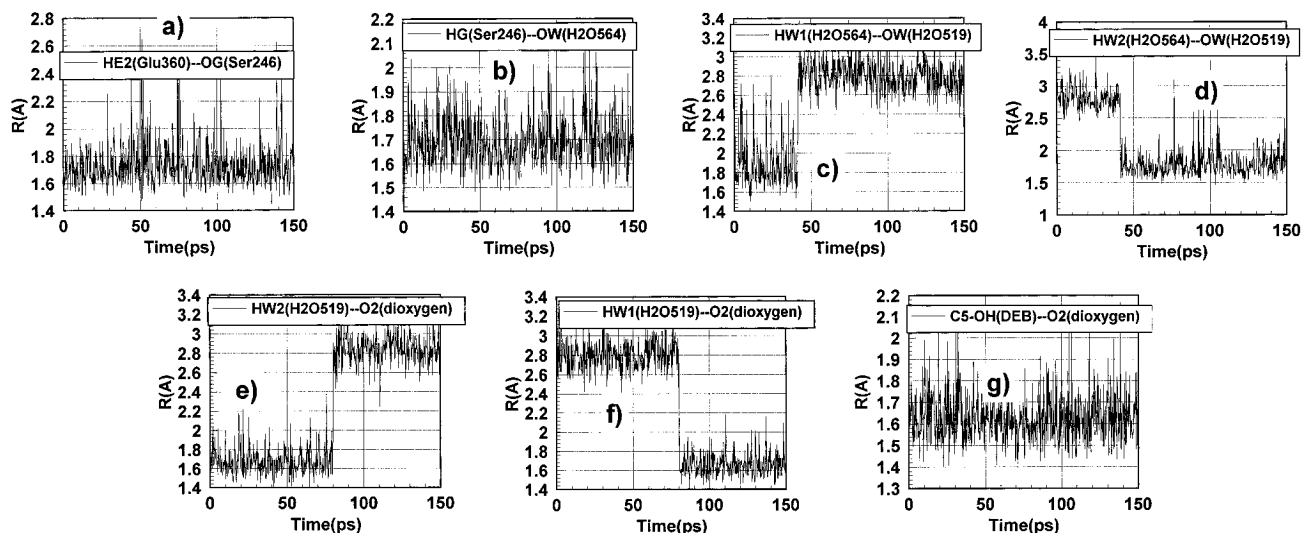


**Figure 10.** Distance time series illustrating the temporal evolution of the connectivity between Glu 360 in the putative protonated form and the bound dioxygen ligand: (a) HE2(Glu 360)---OG(Ser 246); (b) HG(Ser 246)---OW(H2O564); (c) HW1(H2O564)---OW(H2O519); (d) HW2(H2O564)---OW(H2O519); (e) HW2(H2O519)---O2(dioxygen-atom) TWR350; (f) HW1(H2O519)---O2(dioxygen atom) TWR350; (g) C5-OH(H37 of DEB)---O2(dioxygen atom) TWR350. TWR notation is the residue name assigned to the modeled twice reduced dioxygen bound heme species.

C5-OH of the substrate. Moreover, there is a contiguous pathway to the terminal oxygen atom from the protonated Glu 360 via Ser 246 through H2O564 and H2O519. This network differs from that involving the unprotonated Glu, in that donor and acceptor roles along this pathway have been interchanged. Glu at one end of the proton-donating pathway is a donor, Ser-OH is an acceptor, and the bound waters have reoriented to change their roles. In this transient form of the proposed proton-donating pathway, the hydrogen bond connectivity between Glu 360 and the terminal oxygen of the dioxygen ligand is even more robust than in the deprotonated form, in that the H2O564---H2O519 hydrogen bond linkage is better maintained. Figure 10a-g shows the time series associated with this simulation in a manner similar to that done for the unprotonated Glu. Panels a and b of this figure show that a constant hydrogen bond linkage is maintained between the proton on Glu 360 and the Ser 246 hydroxyl oxygen and that in turn this hydroxyl hydrogen is hydrogen bonded to the oxygen of H2O564. Panels c and d show that a hydrogen-bonded link is maintained between the hydrogens of H2O564 and the oxygen of H2O519, although

there are switches between the two hydrogens involved in hydrogen bonding to the oxygen of H2O 519, during the course of the simulation. Finally, panels e and f shows that one of the two hydrogens of H2O519 is always hydrogen bonded to the distal terminal oxygen atom (O2), and panel g shows that a second hydrogen bond to the terminal oxygen atom is formed with the substrate (the C5-OH DEB) itself.

The finding of a robust H-bonded network connecting the terminal oxygen atom of the dioxygen ligand and the Glu in both its protonated and unprotonated forms, as illustrated in Figure 11, lends additional credence to its proposed role as a proton donor and to the plausibility of the switching mechanism of proton transfer, with the Glu picking up a proton from the ultimate donor and delivering it to the distal oxygen atom. Such a mechanism could provide a facile proton transport route with relatively small energy barriers for the transfer process.

The important role assigned to Glu 360 and other residues such as Ser 246 in the proton transfer network crucial to compound I formation can be further assessed by determining

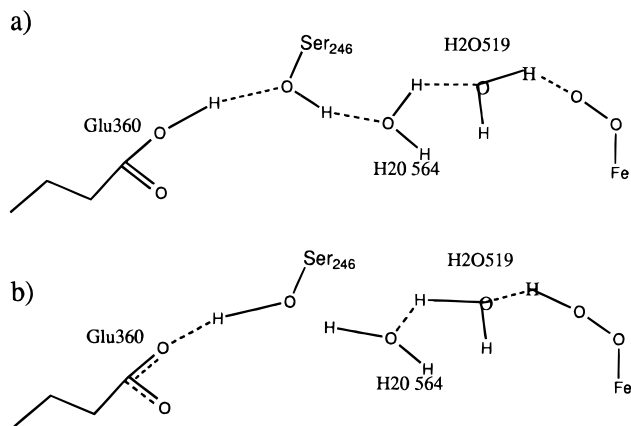


**Figure 11.** Stable H-bonding networks found in the (a) protonated and (b) unprotonated Glu form of the enzyme. The existence of this network in both forms provides support for a proposed switching mechanism resulting in facile proton transfer from the transiently protonated Glu 360 to the terminal oxygen atom of the dioxygen ligand.

the effect on product formation of site specific mutations of these residues.

**Ferryl Oxygen–Heme Substrate-Bound State.** In the previous sections, we have shown how simulations of the transient twice reduced dioxygen species of P450eryF can provide new direct insight into the mechanism of formation of compound I, using methods and procedures validated by comparisons with the known crystal structure of the substrate-bound ferric form of P450eryF. Another opportunity to assess the validity of the methods used to simulate the transient substrate-bound twice reduced dioxygen species is provided by the known experimental hydroxylation profile of 6-DEB by compound I of P450eryF. Using the same simulation conditions we have calculated this profile for the 6-DEB substrate in the putative ferryl state of the enzyme and compared the results with experiment.

It is known that enzymatic conversion by this species of the large natural substrate of WT P450eryF is efficient in that all reduction equivalents result in completely stereo- and regiospecific 6*S*-hydroxylated 6-DEB. The calculated hydroxylation profile is a sensitive function of the enzyme–substrate dynamics since a major geometric criterion for the calculated regiospecificity is deduced from the dynamics of the enzyme–substrate complex. As in the simulations of the twice reduced dioxygen state just described, the coordinates of the known structure of the ferric–heme substrate-bound state were used as a starting point for the ferryl–oxygen species and no bound waters were added or removed in constructing the ferryl state.

During both energy optimization and the subsequent 140 ps of equilibrated MD simulations, the changes in the 6-DEB orientation in the substrate binding site from its starting configuration were small, the substrate being constrained by its numerous van der Waals contacts with hydrophobic residues and hydrogen bonds via bound waters to polar residues. The coordinates saved at 0.25 ps intervals during the MD trajectory were used to calculate distances and angles between all possible H atom abstraction sites of the substrate and the ferryl oxygen atom. As shown in Table 2, there were only five H atoms, of the many shown in Figure 4b, for which there was a nonzero number of sampled structures in which the chosen steric criteria were fulfilled, i.e., a distance equal to or less than 3.5 Å and an angle within 45° of linear. Given in Table 2 for these five “reactive” H atoms, in the column labeled “steric %”, is the number as well as percentage of the sampled structures in which a particular H*n* position satisfied these criteria. If only these

**Table 2.** Predicted Hydroxylation of 6-DEB from Simulations of the Ferryl Form of P450eryF

atom	sum	steric %	steric+ electronic%
H6	350	62.7	100
H24	1	0.2	
H25	3	0.5	
H26	2	0.4	
H29	202	36.2	
total no. of reactive configs	558	100	

**Table 3.** Relative Energetics of 6-DEB Radicals Resulting from Hydrogen Extraction as Determined from an AM1/G94 Optimization

DEB radical site <sup>a</sup>	energy (hartree)	Δ <i>E</i> (kcal/mol)
H24	−0.4791	10.6
H26	−0.4738	13.9
H29	−0.4755	12.8
H6	−0.4959	0.0

<sup>a</sup> The radical site is denoted by the hydrogen atom which would be extracted to generate a radical at this site. H24 and H26 are primary hydrogens attached to the C6 methyl group, and H29 is a primary hydrogen attached to the C8 methyl. H6 is a tertiary hydrogen attached to the C6 carbon (cf. Figure 4b).

steric factors were used, this column would be used to directly predict hydroxylation regiospecificity. However, as shown previously, the observed hydroxylation profile is not only a function of the accessibility of the substrate hydrogens to the reactive ferryl oxygen but is also modulated by the relative radical energetics.

Table 3 presents the calculated relative energetics of the radicals at the five aliphatic hydrogen sites shown from dynamics trajectories to be accessible to abstraction by the reactive P450-bound ferryl oxygen. Of these five H atoms, the C6-H is a tertiary hydrogen, and the remainder of the hydrogens are primary hydrogen atoms of methyl groups. H24, H25, and H26 are on the methyl group attached to the C6 carbon, and H29 is on the methyl group attached to the C8 carbon.

The results indicate large energy differences between these primary and tertiary sites, comparable to those reported from AM1 results for simple aliphatic species. Previous calculations of the energy differences between primary and tertiary aliphatic radicals using ab initio and AM1 semiempirical estimates were 3 and 10 kcal mol<sup>−1</sup>, respectively.<sup>20</sup> Despite these disparities, both of these energy differences would result in exclusive formation of a tertiary radical based on an assumed Boltzmann-like thermodynamic distribution of radicals and kinetic partitioning of products based on this radical distribution. Thus, using even a conservative lower bound estimate of 3 kcal mol<sup>−1</sup> from the ab initio results as the energy difference between tertiary and primary radicals, together with the steric criteria obtained, results in prediction of exclusive production of 6*S*-hydroxylated product by the enzyme as indicated in Table 2 (cf. Steric/Electronic %) in agreement with the observed completely regio- and stereospecific hydroxylation for this native substrate of cytochrome P450eryF.<sup>2</sup>

## Conclusions

In this work, we have simulated the dynamic behavior of three substrate-bound species in the enzymatic cycle of cytochrome P450eryF: the ferric species, the ferryl form, and the twice reduced dioxygen species based on the crystal structure of the ferric–heme substrate-bound form. The same simulation conditions and approximations were employed in all three simulated states of the enzyme. The main aims of these studies were to use the results obtained for the first two species to

validate the methods used by comparisons with experiment and to use the results for the twice reduced dioxygen bound species to probe the validity of the proton-assisted mechanism of compound I formation from it.

The simulation conditions used for the ferric–heme substrate-bound species led to dynamic behavior in reasonable accord with the crystal structure results. Under the same conditions the calculation of the hydroxylation of the 6-deoxyerythronolide substrate by the ferryl form of P450eryF led to the prediction of a single 6S-hydroxylation product in complete agreement with experiment. The results obtained for both the ferric and compound I forms of this enzyme thus lend credence to the methods used in the simulations of the transient twice reduced dioxygen bound P450eryF.

It is known from experimental studies of P450cam that the steps following the second reduction of the dioxygen bound complex involve on the order of two protons as determined from proton-isotope effects and the formation of water in addition to oxidized product.<sup>9</sup> These experimental observations are consistent with the proposed proton-assisted formation of the reactive ferryl species from the twice reduced dioxygen form depicted in Figure 2. Additional experimental evidence for this mechanism is difficult to obtain, however, given the transient nature of both of these species. The MD simulation of the twice reduced dioxygen bound state of P450eryF performed here reveals for the first time two hydrogen bonds preferentially formed to the terminal oxygen of the bound dioxygen that persist throughout a significant fraction of a 150 ps simulation. This hydrogen-bonding pattern corresponds to an incipient complex leading to splitting out water and formation of a ferryl complex. The geometric time series analysis indicates that incipient complex is preferred to the alternative pattern of one H-bond to each of the two ligand oxygen atoms that would lead to H<sub>2</sub>O<sub>2</sub> formation, i.e., one preferential hydrogen bond to each of the distinct oxygen atoms. Although such classical simulations do not investigate the actual dioxygen bond breaking process, the double protonation found favoring the terminal oxygen corresponds to a reaction complex that can be reasonably inferred to lead to formation of water and compound I by dioxygen bond weakening and rapid bond cleavage. It thus provides convincing additional evidence for the proton-assisted dioxygen bond cleavage mechanism of formation of compound I shown in Figure 2.

In addition to the observation of preferential double proton donation to the terminal oxygen atom, a dynamically stable hydrogen-bonding network pattern can be traced in this simulation that links this oxygen atom through H2O519, Ala 241, H2O564, and the Ser 246 hydroxyl to the Glu 360. This network persists, with roles interchanged, in the substrate-bound twice reduced dioxygen simulation with the protonated form of Glu 360 proposed as the proton donor by a rotation of this side chain after transient proton donation to it from solvent.

The finding of a robust H-bonded network connecting the terminal oxygen atom of the dioxygen ligand and the Glu in both its protonated and unprotonated forms, as summarized in Figure 11, provides support for a plausible proton transfer mechanism and the role of such a network in it. This figure illustrates that a proton can be donated from the Glu to the terminal oxygen ligand atom via a hydrogen bond switching mechanism. Such a mechanism could then provide in principle a facile proton transport route with relatively small energy barriers for the transfer process.

If the hypothesized mechanism of formation of compound I proposed here is correct, disruption of the proton transfer system would decrease enzymatic efficiency. It is already known that a substrate modification removing the C5-OH group prevents product formation in keeping with its importance in proton donation to the distal oxygen atom.<sup>1,2</sup> In a complementary fashion, the important role assigned here to Glu 360 and other residues such as Ser 246 in the proton transfer network crucial to compound I formation can be further assessed by determining the effect on product formation of site specific mutations of these residues.

**Acknowledgment.** The authors wish to thank Dr. Tom Poulos for kindly sharing crystallographic data on P450eryF. The authors also gratefully acknowledge support of NIHGM 27943 and a grant of NSF supercomputer time on C90, T3D, and J-90 platforms.

**Supporting Information Available:** Charge and AMBER 4.1 atom type assignments for the twice reduced dioxygen bound heme state and the 6-DEB substrate (5 pages). Ordering information is given on any current masthead page.

JA954101M